Nuclear Instruments and Methods in Physics Research B 269 (2011) 2709–2714

Contents lists available at SciVerse ScienceDirect

Nuclear Instruments and Methods in Physics Research B

journal homepage: www.elsevier.com/locate/nimb

Xe-implanted zirconium oxycarbide studied by variable energy positron beam

N. Djourelov [a,*], G. Gutierrez [b], H. Marinov [a], E. Popov [a], N. Toulhoat [b,c], N. Moncoffre [b], Y. Pipon [b,d], P. Nédélec [b]

[a] Institute for Nuclear Research and Nuclear Energy, Bulgarian Academy of Sciences, 72 Tzarigradsko Chaussee Blvd., BG-1784 Sofia, Bulgaria
[b] Université de Lyon, Laboratoire IPNL, UCB Lyon 1, Bâtiment Paul Dirac 4, rue Enrico Fermi, 69622 Villeurbanne Cedex, France
[c] Commissariat à l'Energie Atomique CEA/DEN, Centre de Saclay, 91191 Gif sur Yvette Cedex, France
[d] Institut Universitaire de Technologie (IUT), Université Claude Bernard Lyon 1, 94 Bd. Niels Bohr, 69622 Villeurbanne Cedex, France

ARTICLE INFO

Article history:
Received 16 May 2011
Received in revised form 27 July 2011
Available online 3 September 2011

Keywords:
Zirconium oxycarbide
Xenon implantation
Positron beam
Defects
Bubbles

ABSTRACT

The effect of annealing on defects and the formation of Xe bubbles were investigated in zirconium oxycarbide implanted with 800-keV $^{136}Xe^{2+}$ ions at two fluences 1×10^{15} and 1×10^{16} Xe/cm^2. Doppler broadening technique combined with slow positron beam was used. The analysis of the *S* depth profiles and *S*–*W* maps revealed that in the as-implanted samples at both fluences Xe bubbles are not formed. The post-implantation annealing of the samples implanted at 1×10^{16} Xe/cm^2 caused formation of Xe bubbles. The response of the lower implantation dose samples to this post implantation annealing was found rather complicated and is discussed.

1. Introduction

ZrC is one of the high refractory materials and therefore it is selected as a potential material for some components of the reactor cores in the frame of the Generation-IV International Project [1]. Besides its excellent mechanical properties and its good thermal stability, ZrC demonstrates a high resistance to fast neutrons irradiation and a high capability for fission product retention [2].

Xenon is a volatile fission product the thermally stimulated diffusion behaviour of which is of great importance for the performance of ZrC as a cladding material. In many materials Xe segregates and forms bubbles as a result of its very low solubility [3–5]. The technique of ion implantation is widely used to simulate the accumulation of fission products in order to perform averaged studies of the fission gas release and of the microstructure evolutions under different treatment. The size of the formed bubbles in silicon implanted with Xe at 5×10^{15} Xe/cm^2 has been measured by defocused transmission electron microscopy (TEM) with a lower limit of ~1.8 nm [6]. In UO_2 implanted at 6×10^{12} Xe/cm^2, Xe bubbles have been observed with a size of 0.8 nm [7]. Secondary ion mass spectrometry (SIMS) [8] and Rutherford BackScattering (RBS) provide information for implanted ion profiles.

The processes of ion implantation as well as of neutron irradiation are accompanied by formation of defects. Positron annihilation spectroscopy (PAS) is a powerful tool to study defects in materials. The slow positron beam (SPB) technique is based on injection of positrons with controlled variable energy to achieve depth profiling of defects (for a review see [9]). There are great number of application of SPB to study vacancy clusters and bubbles in He-implanted silicon [10–12] and He-implantation in other materials. Few SPB studies concern Xe-implantation in SiO_2 [13], SiC [14] and spinel [15].

In the present work, Doppler broadening with SPB is used to study the evolution of defects in $ZrC_{0.95}O_{0.05}$ after Xe-implantation and post-implantation annealing.

2. Experimental

2.1. Samples

$ZrC_{0.95}O_{0.05}$ powders were synthesized at SPCTS in Limoges by carbothermal reduction of zirconia [16]. The powders were sintered in the form of pellets (Ø = 2 cm) at 2225 K under vacuum with an applied load of 100 MPa using spark plasma sintering (SPS) at the University of Toulouse [16]. Pellets density was measured to be $\rho = 6.28$ g/cm^3 using Archimedes's method. The pellets were cut into several samples of $7 \times 7 \times 2$ mm^3 and polished to micron. In order to anneal the subsurface defects introduced by the polishing and to limit sample degassing during high temperature annealing, the annealing was performed in two successive steps at 1273 K for 10 h in a tubular furnace and at 1673 K for 3 h in an induction furnace. After that, the mean grain size was

* Corresponding author.
E-mail address: nikdjour@inrne.bas.bg (N. Djourelov).

0168-583X/$ - see front matter © 2011 Elsevier B.V. All rights reserved.
doi:10.1016/j.nimb.2011.08.022

controlled by scanning electron microscopy (SEM) and determined to be 1.5 ± 0.5 μm.

2.2. Sample implantation and annealing

The polished samples were implanted with $^{136}Xe^{2+}$ ions at room temperature at the Institute of Nuclear Physics of Lyon. Samples have been implanted at energy of 800 keV at two implantation fluences of 1×10^{15} and 1×10^{16} Xe/cm^2. The xenon distribution with a projected range of R_{Xe} = 160 nm and a number of displacement per atoms (dpa) peaking at R_d = 110 nm in the implanted samples obtained by SRIM [17] are shown in Fig. 1. After implantation, some samples were annealed under secondary vacuum (5×10^{-7}–5×10^{-6} mbar) during 3 h at 1675 K. Additional subsequent thermal annealing was carried out under vacuum (1×10^{-6}–5×10^{-6} mbar) at 2073 K during several annealing times using induction heating.

Table 1 summarizes the characteristics of the Xe implantation, and of the post-polishing and post-implantation annealing. The table also includes some results from the spectra analysis discussed in Section 2.4.

2.3. Positron beam setup

The SPB measurements were carried out with a Canberra high purity Ge detector (HPGe) with a resolution G = 1.17 keV (FWHM) at the 514 keV line of ^{85}Sr on the direct current slow e^+ beam in Sofia (the former Ghent beam). Details on this e^+ beam can be found elsewhere [18]. The HPGe detector was set up at the sample position perpendicular to the beam axis at a distance of 4 cm from the sample. Due to the fact that the e^+ spot size of ~6 mm was comparable with the sample size, special arrangements were made to ensure that e^+, which did not hit the sample, annihilate far from

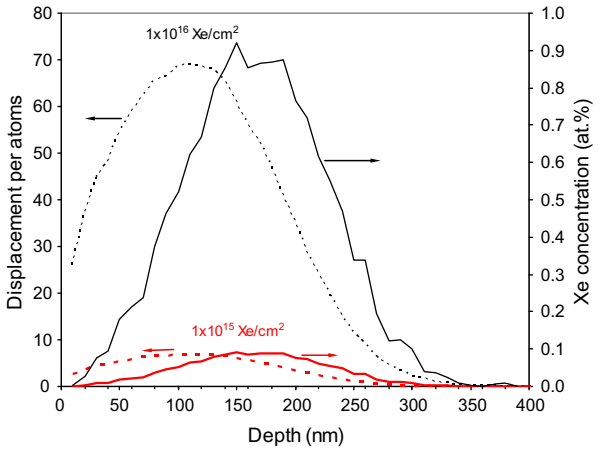

Fig. 1. Depth distribution of implanted Xe at two fluences and displacement per atom as obtained by SRIM.

Table 1
Sample, implantation fluence, pre- and post-implantation treatment. Thickness, Z_d, S_d parameter and positron diffusion length L_+ for the damaged layer as obtained by VEPFIT. The slope, R, for the S–W linear fit.

Sample	Polished	Post-polishing annealing	Implantation (Xe/cm^2)	Post-implantation annealing time (h)		Damaged layer			
				At 1675 K	At 2075 K	Z_d (nm)	S_d ± 0.0007	L_+ (nm)	R ± 0.03
P	+	–	–	–	–	18 ± 1	0.5110	5 ± 0.5	0.79
P_A	+	+	–	–	–	6 ± 0.2	0.5045	5 ± 0.2	0.73
A_0	+	+	1×10^{15}	–	–	162 ± 17	0.5127	27 ± 3	1.36
A_3	+	+	1×10^{15}	3	–	194 ± 7	0.5690	33 ± 1	2.05
A_{31}	+	+	1×10^{15}	3	1	201 ± 15	0.5655	56 ± 5	2.01
A_{38}	+	+	1×10^{15}	3	8	193 ± 14	0.5205	23 ± 2	1.58
A_{312}	+	+	1×10^{15}	3	12	171 ± 14	0.5285	19 ± 2	1.75
A_{316}	+	+	1×10^{15}	3	16	90 ± 6	0.5393	9 ± 0.4	1.89
B_0	+	+	1×10^{16}	–	–	85 ± 7	0.5270	14 ± 1	1.38
B_3	+	+	1×10^{16}	3	–	39 ± 3	0.5458	9 ± 1	1.83
B_{31}	+	+	1×10^{16}	3	1	92 ± 4	0.5851	22 ± 1	1.82
B_{316}	+	+	1×10^{16}	3	16	53 ± 2	0.5901	17 ± 1	1.83

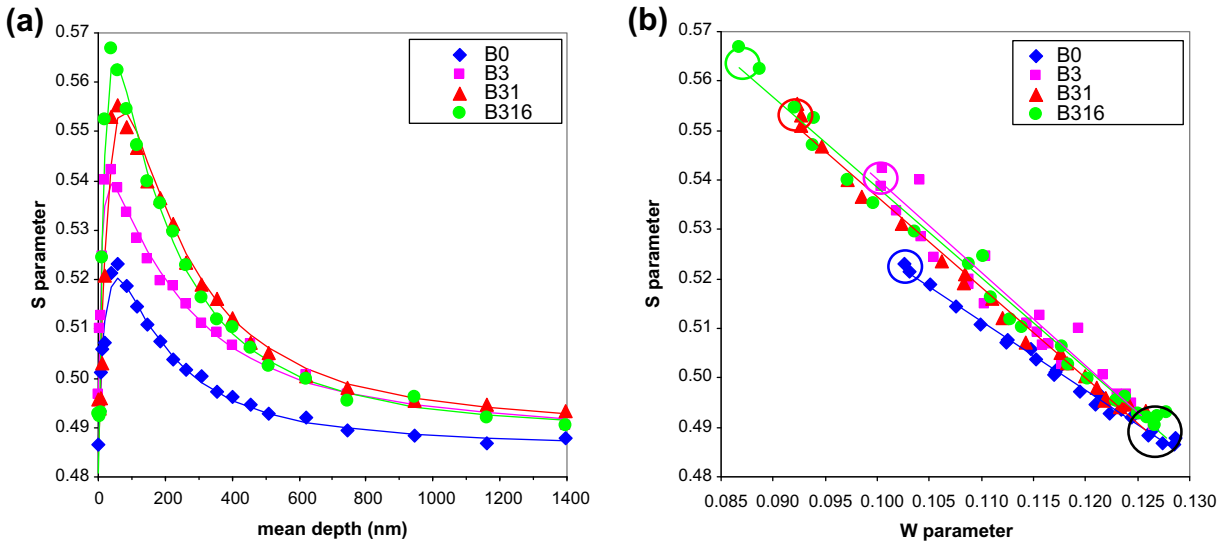

Fig. 2. Depth profiles of S parameter (a) and S vs. W (b) for as-implanted at 1×10^{16} Xe/cm^2 and post-implantation annealed samples. The curves are the best fits obtained by VEPFIT (a) and linear fits (b). The errors are of the order of the point sizes. The circles in (b) represent the extreme S–W.